

# *Supporting Information*

## **Simultaneous Thermal Stability and Ultrahigh Sensitivity of Heterojunction SERS Substrates**

**Lingwei Ma <sup>1</sup>, Jinke Wang <sup>1</sup>, Hanchen Huang <sup>2,\*</sup>, Zhengjun Zhang <sup>3,\*</sup>, Xiaogang Li <sup>1</sup> and Yi Fan <sup>4</sup>**

<sup>1</sup> Institute of Advanced Materials & Technology, University of Science and Technology Beijing, Beijing 100083, China; mlw1215@ustb.edu.cn (L.M.); wjkgege@126.com (J.W.); lixiaogang@ustb.edu.cn (X.L.)

<sup>2</sup> College of Engineering, University of North Texas, Denton, TX 76207, USA

<sup>3</sup> Key Laboratory of Advanced Materials, School of Materials Science and Engineering, Tsinghua University, Beijing 100084, China

<sup>4</sup> Jiangsu Key Laboratory for Premium Steel Material, Nanjing Iron and Steel Co., Ltd., Nanjing 210035, China; fanyi@njsteel.com.cn

\* Correspondence: Hanchen.Huang@unt.edu (H.H.); zjzhang@tsinghua.edu.cn (Z.Z.)

## The thickness optimization of Al<sub>2</sub>O<sub>3</sub> layer on top of AgNRs

Our choice of Al<sub>2</sub>O<sub>3</sub> thickness is based on the following two considerations. First, Al<sub>2</sub>O<sub>3</sub> thickness needs to be sufficiently small to avoid the excessive coverage of Ag surfaces. Second, it needs to be large enough to maximize the thermal stability. With these two considerations, Al<sub>2</sub>O<sub>3</sub> layers of 6, 8, 10, 12, 15 and 20 nm were deposited over AgNRs, and these hybrid substrates are denoted as AgNRs-6Al<sub>2</sub>O<sub>3</sub>, AgNRs-8Al<sub>2</sub>O<sub>3</sub>, AgNRs-10Al<sub>2</sub>O<sub>3</sub>, AgNRs-12Al<sub>2</sub>O<sub>3</sub>, AgNRs-15Al<sub>2</sub>O<sub>3</sub> and AgNRs-20Al<sub>2</sub>O<sub>3</sub>, respectively. Figures S1a-S1b show typical SEM micrographs of AgNRs and AgNRs-10Al<sub>2</sub>O<sub>3</sub>, separately. Both substrates possessed tilted and closely arranged nanorod morphologies with sharp corners and edges. In view of the ultrathin feature of Al<sub>2</sub>O<sub>3</sub> capping, it is hard to be differentiated from the SEM resolution. To this end, HRTEM analysis was adopted to offer visual evidences of the Al<sub>2</sub>O<sub>3</sub> capping. Figures S1c-S1e display representative HRTEM images of AgNRs capped with Al<sub>2</sub>O<sub>3</sub> layers of 8, 10 and 20 nm, respectively. As can be seen, these Al<sub>2</sub>O<sub>3</sub> layers with diverse thickness were only located at the top surfaces of AgNRs, and the side surfaces were largely exposed, which were essential to directly adsorb molecules for SERS amplification.

We then assessed the SERS efficiency of various AgNRs-Al<sub>2</sub>O<sub>3</sub> substrates. Figure S2a presents the SERS spectra of  $1 \times 10^{-6}$  M MB on AgNRs-Al<sub>2</sub>O<sub>3</sub> substrates with different capping thickness. As expected, in light of the enhance separation between Ag tips and adsorbates introduced by Al<sub>2</sub>O<sub>3</sub> capping, MB Raman signals decreased monotonously with the increase of Al<sub>2</sub>O<sub>3</sub> thickness. Herein, the 1622 cm<sup>-1</sup> Raman peak with strong intensity was chosen to quantify the oxide capping effect on SERS activity. For each sample, the peak value was normalized to that on bare AgNRs to facilitate comparison (see Figure S2b). To be specific, the SERS intensities of MB on AgNRs-Al<sub>2</sub>O<sub>3</sub> substrates with 6 nm to 12 nm capping occupied approximately 80% to 70% relative to those on bare AgNRs, and declined moderately to 62% and 56% with further Al<sub>2</sub>O<sub>3</sub> deposition to 15 nm and 20 nm, separately. Even though there was some signal degradation after Al<sub>2</sub>O<sub>3</sub> capping, these hybrid substrates still exhibited satisfactory SERS enhancement, which was owing to the exposed side surfaces of AgNRs that could directly interact with target molecules.

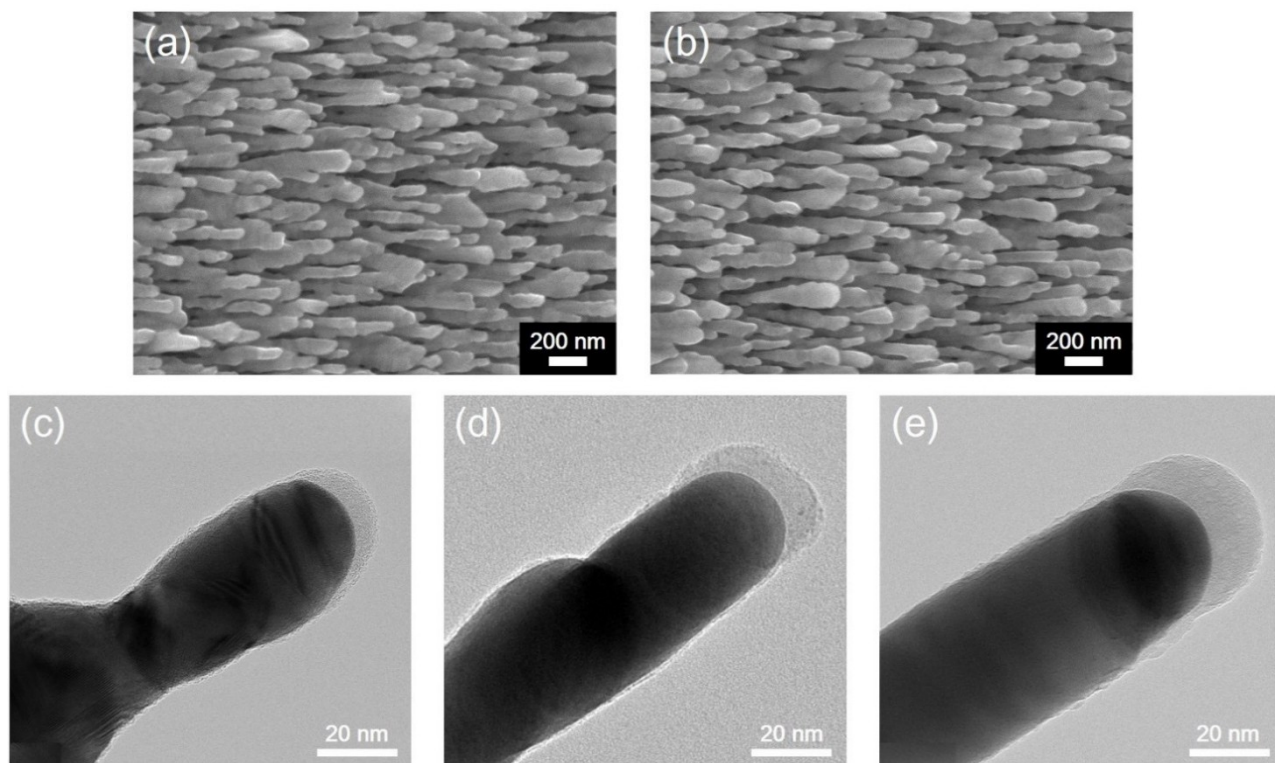


Figure S1. SEM images of (a) uncapped AgNRs and (b) AgNRs-10Al<sub>2</sub>O<sub>3</sub> substrates; HRTEM images of AgNRs capped with Al<sub>2</sub>O<sub>3</sub> layers of (c) 8, (d) 10 and (e) 20 nm, respectively.

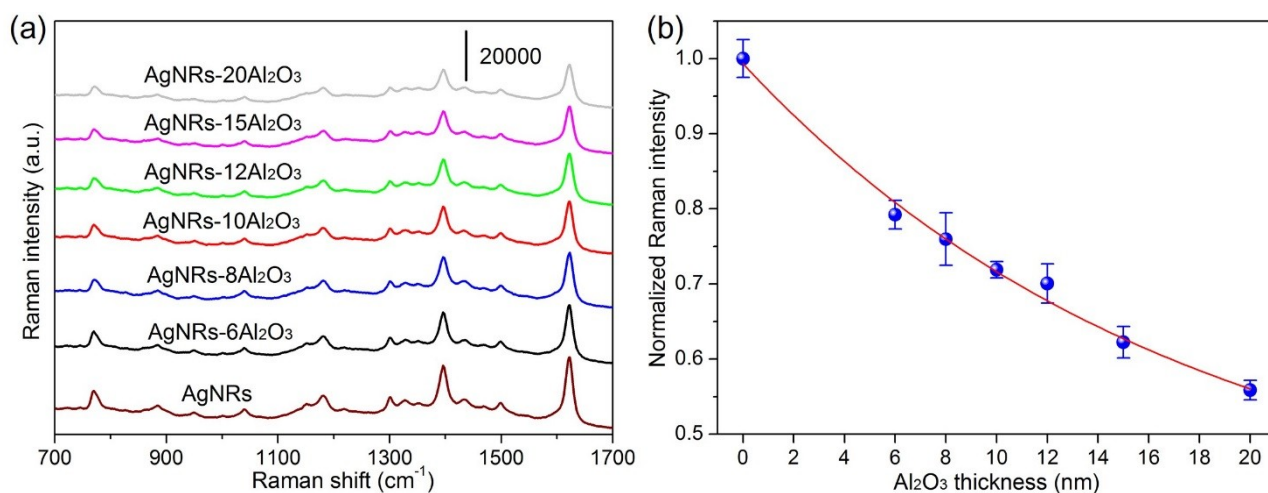


Figure S2. (a) SERS spectra of 1×10<sup>-6</sup> M MB adsorbed on bare AgNRs and on AgNRs-Al<sub>2</sub>O<sub>3</sub> substrates with different capping thickness; (b) The normalized intensities of 1622 cm<sup>-1</sup> Raman peak of 1×10<sup>-6</sup> M MB molecules as a function of the Al<sub>2</sub>O<sub>3</sub> thickness of different AgNRs-Al<sub>2</sub>O<sub>3</sub> substrates.

In spite of the slight decay of SERS signals on AgNRs after Al<sub>2</sub>O<sub>3</sub> deposition, the capping layers we introduced here were mainly applied to enhance the corresponding thermal stability. It is known that the high-

temperature robustness of nanostructures relies on their resistance to coarsening. If the molecule diffusion of metal surfaces can be restricted, nanostructures might be stabilized at elevated temperatures. Figure S3 illustrates the morphologies of AgNRs and diverse AgNRs- $\text{Al}_2\text{O}_3$  substrates after annealing at 150 °C and 200 °C for 15 min. Evidently, the uncapped AgNRs fused seriously into irregular aggregations after heating, which were not applicable for high-temperature detections. On the other hand, this situation was sharply relieved for AgNRs- $\text{Al}_2\text{O}_3$  samples. Specifically, even if the  $\text{Al}_2\text{O}_3$  coating was only 8 nm for AgNRs-8 $\text{Al}_2\text{O}_3$ , it could prevent the surface diffusion of AgNRs from tips to sides, and thereby the substrate maintained its shape with only small deformation at 150 °C. At 200 °C, the film collapsed to some extent while there were still recognizable nanorod shapes. Subsequently, by depositing 10 nm and 20 nm  $\text{Al}_2\text{O}_3$  onto AgNRs, the substrates exhibited no discernible morphology variation at 150 °C and coarsened slightly at 200 °C. Therefore, we could maximize the resistance to surface diffusion by capping the top surfaces of AgNRs with  $\text{Al}_2\text{O}_3$ , and enhance the thermal stability of AgNRs- $\text{Al}_2\text{O}_3$  films accordingly.

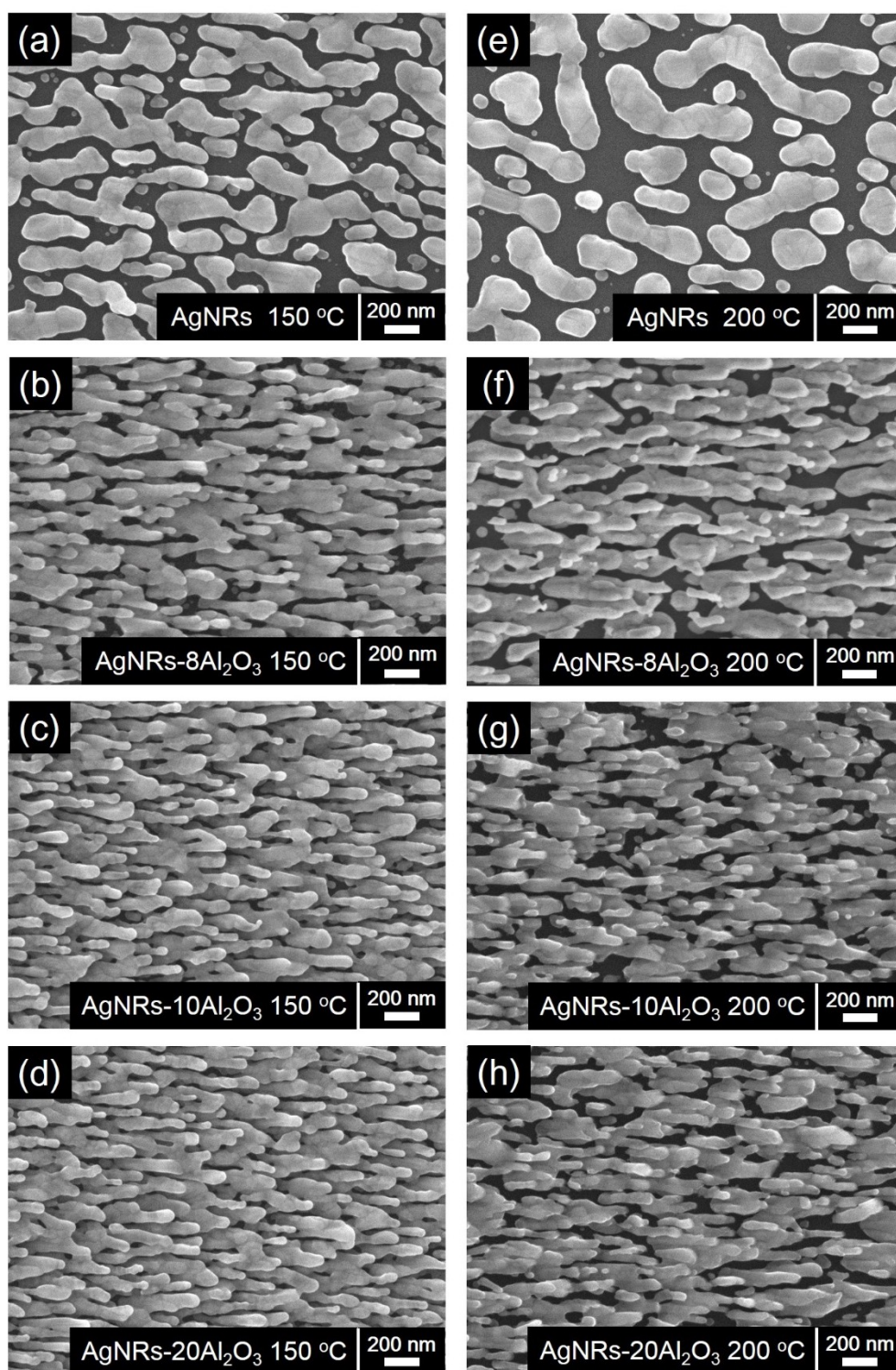


Figure S3. SEM images of AgNRs and different AgNRs- $\text{Al}_2\text{O}_3$  substrates after annealing at 150 °C and 200 °C for 15 min.

To characterize *in situ* the melting procedures and structural changes of AgNRs- $\text{Al}_2\text{O}_3$  substrates, we measured the reflectivity changes of SERS substrates upon annealing. Figure S4 thoroughly analyzes the



melting behaviors of different AgNRs- $\text{Al}_2\text{O}_3$  substrates from 100 °C to 250 °C. For AgNRs-6 $\text{Al}_2\text{O}_3$  and AgNRs-8 $\text{Al}_2\text{O}_3$ , their reflectivity began to change at ~125 °C and varied sharply at ~180 °C, which might due to the collapse of nanorods. As for the hybrid substrates capped with thicker  $\text{Al}_2\text{O}_3$  layers of 10-20 nm, their morphology maintained well to ~200 °C. As a result, a 10 nm  $\text{Al}_2\text{O}_3$  protection layer could restrict the morphological changes of AgNRs at temperatures as high as 200 °C, and AgNRs-10 $\text{Al}_2\text{O}_3$  possessed minimal degradation in SERS enhancement than the hybrids capped with thicker  $\text{Al}_2\text{O}_3$  layers. We hence recommend AgNRs-10 $\text{Al}_2\text{O}_3$  film in this study to guarantee both the stability and sensitivity characters of SERS substrates.

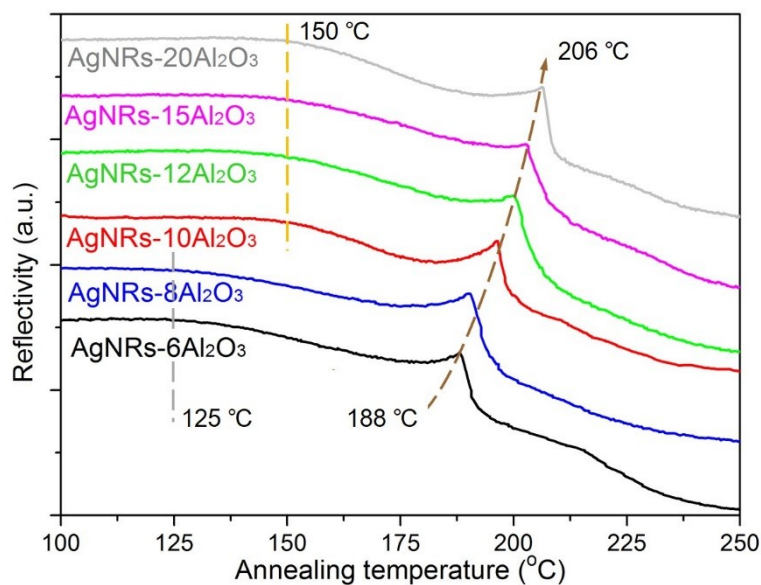


Figure S4. The reflectivity changes of different AgNRs- $\text{Al}_2\text{O}_3$  substrates upon annealing from 100 °C to 250 °C.

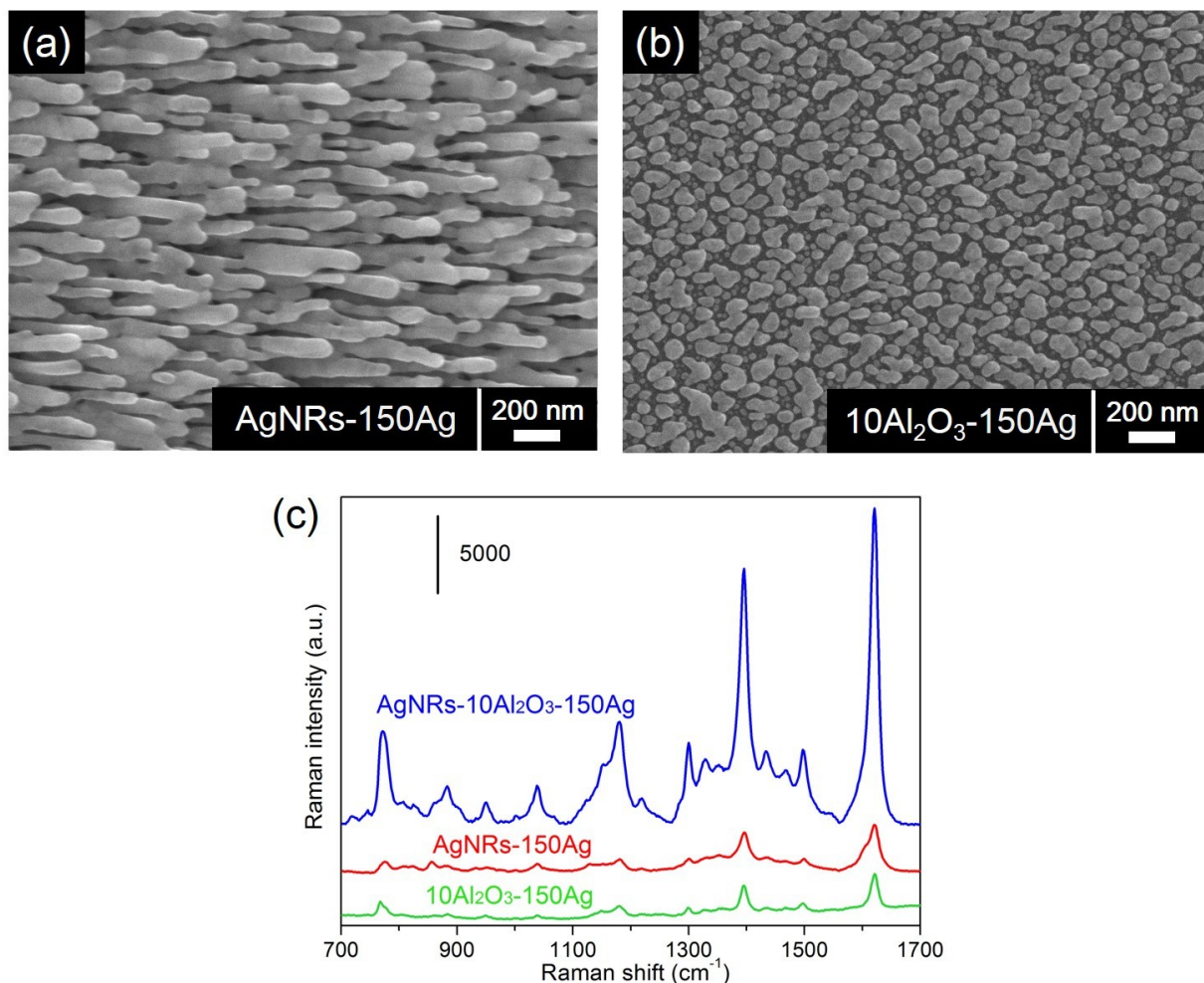


Figure S5. SEM images of (a) AgNRs-150Ag and (b) 10Al<sub>2</sub>O<sub>3</sub>-150Ag substrates; (c) SERS spectra of  $1 \times 10^{-6}$  M MB molecules adsorbed on AgNRs-10Al<sub>2</sub>O<sub>3</sub>-150Ag, AgNRs-150Ag and 10Al<sub>2</sub>O<sub>3</sub>-150Ag substrates, separately.

### The calculation of SERS enhancement factor

Methylene blue (MB) molecules were used to calculate the SERS enhancement factor (EF) of AgNRs-Al<sub>2</sub>O<sub>3</sub>-Ag arrays with 150 nm additional Ag. The SERS spectra of  $1 \times 10^{-6}$  to  $1 \times 10^{-10}$  M MB molecules were first collected on the substrates, as shown in Figure 3a and Figure 4a. Figure 4b plots the Raman peak signals at  $1622 \text{ cm}^{-1}$  against MB concentrations, which increased gradually and became saturated.

The SERS spectrum of  $1 \times 10^{-6}$  M MB on SERS substrate and the Raman spectrum of 0.1 M MB in solution were used to calculate the SERS EF of AgNRs-Al<sub>2</sub>O<sub>3</sub>-Ag arrays with 150 nm additional Ag. The EF was calculated by<sup>[1, 2]</sup>:

$$EF = \frac{I_{SERS}}{I_{Ref}} * \frac{N_{Ref}}{N_{SERS}}$$

In this formula,  $I_{SERS}$  is the enhanced intensity of the adsorbed MB molecules on AgNRs- $Al_2O_3$ -Ag arrays, and  $I_{Ref}$  is the integrated spontaneous Raman scattering intensity collected from the MB molecules in solution.  $N_{SERS}$  is the number of the molecules covering the SERS substrate under the laser spot, and  $N_{Ref}$  is the number of MB molecules in aqueous solution excited by the laser. The strong Raman peak intensity at  $1622\text{ cm}^{-1}$  was used for EF calculation.

For the Raman equipment in this study, the laser light is focused onto a region with a diameter of  $80\text{ }\mu\text{m}$ . To calculate the value of  $N_{SERS}$ , MB molecules were assumed to be deposited onto the substrate under the ideal condition that they were absorbed on the substrate surface as a monolayer. With the calculated area of a single MB molecule of  $1.29 \times 10^{-18}\text{ m}^2$  [3], the value of  $N_{SERS}$  under the laser excitation is approximately  $3.9 \times 10^9$ . The focal volume of the Raman spectrometer is about  $5.0 \times 10^6\text{ }\mu\text{m}^3$ . Correspondingly, the  $N_{Ref}$  is calculated to be  $3.0 \times 10^{15}$  by multiplying volume, concentration of MB solution and an Avogadro constant ( $N_A=6.02 \times 10^{23}\text{ mol}^{-1}$ ). The  $1622\text{ cm}^{-1}$  intensity of  $1 \times 10^{-6}\text{ M}$  MB on AgNRs is about 22350 counts, and that of  $0.1\text{ M}$  MB in solution is 187 counts, providing an EF of approximately  $1.3 \times 10^8$ .

## References:

- [1] S. Xu, Y. Zhang, Y. Luo, S. Wang, H. Ding, J. Xu and G. Li, Ag-decorated  $TiO_2$  nanograss for 3D SERS-active substrate with visible light self-cleaning and reactivation, *Analyst* 138 (2013) 4519.
- [2] J. Yin, Y. Zang, C. Yue, X. He, H. Yang, D. Wu, M. Wu, J. Kang, Z. Wu, J. Li, Multiple coupling in plasmonic metal/dielectric hollow nanocavity arrays for highly sensitive detection, *Nanoscale* 7 (2015) 13495.
- [3] E. El Qada, S. Allen, G. Walker, Adsorption of Methylene Blue onto activated carbon produced from steam activated bituminous coal: A study of equilibrium adsorption isotherm, *Chem. Eng. J.* 124 (2006) 103-110.